

Generation of patient-derived glioblastoma organoids: a comparative study of enzymatic digestion and mechanical fragmentation methods

Authors

Jian Zhang, Jiping Liu, Yanghua Shi,
Lanyang Li, Chen Wang, ...,
Chunhui Cai*, Xinxin Han*

Correspondence

Chunhui Cai, caichunhui@lishengbiotech.com;
Xinxin Han, xxhan@sibs.ac.cn

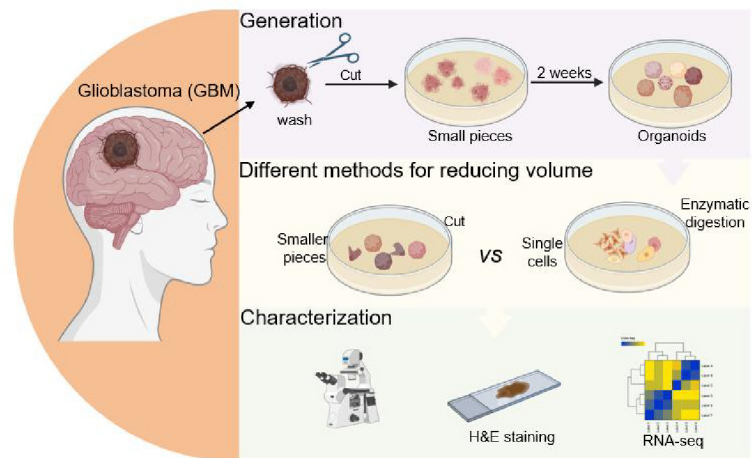
In Brief

In this study, we employed enzymatic digestion and mechanical fragmentation to generate Glioblastoma (GBM) organoids. Utilizing photography, RNA sequencing (RNA-seq), and histological staining, we meticulously documented and compared the morphological and molecular features of the organoids derived from both methods. Our findings underscore the preservation of GBM's key characteristics, including its unique tissue architecture and gene expression patterns.

Highlights

- Successfully generated four patient-derived organoids.
- RNA-seq was used to monitor gene expression changes at various stages of organoid growth.
- Both propagation methods successfully maintain the typical characteristics and immune microenvironment of glioblastoma (GBM) organoids.
- The GBM organoids prepared by mechanical fragmentation retained vascular architecture.

Graphical abstract



Generation of patient-derived glioblastoma organoids: a comparative study of enzymatic digestion and mechanical fragmentation methods

Jian Zhang¹, Jiping Liu¹, Yanghua Shi¹, Lanyang Li¹, Chen Wang¹, Mingjie Rong¹, Bangbao Tao², Hong Tan³, Wei Deng⁴, Chunhui Cai^{1,*}, and Xinxin Han^{1,5,*}

¹ Shanghai Lisheng Biotech, Shanghai 200092, China

² Department of Neurosurgery, Xinhua Hospital, School of Medicine, Shanghai Jiao Tong University, Shanghai 200092, China

³ Department of Anesthesiology, Huashan Hospital, Fudan University, Shanghai, China

⁴ LongHua Hospital, Shanghai University of Traditional Chinese Medicine, Shanghai 200032, China

⁵ Organ Regeneration X Lab, LiSheng East China Institute of Biotechnology, Peking University, Nantong 226299, China

Received: 2 February 2024 / Revised: 29 April 2024 / Accepted: 12 May 2024

ABSTRACT

Glioblastoma (GBM) is a highly aggressive brain tumor characterized by rapid growth and high heterogeneity, posing challenges for fundamental research and personalized drug screening due to the lack of suitable models. GBM organoids serve as an innovative research tool, providing a valuable model for studying the biological characteristics of GBM. In this study, we successfully generated 4 GBM organoids and employed enzymatic digestion and mechanical fragmentation techniques for subsequent cultivation. Through continuous observation, pathological assessment, and RNA sequencing (RNA-seq), we observed that all the organoids generated through both methods demonstrated good growth characteristics. The organoids derived from mechanical fragmentation not only achieved a two-dimensional (2D) area of ~ 1.5 mm² but also exhibited distinct vascular structures. The organoids derived from enzymatic digestion achieved a 2D area of approximately 0.8 mm². Furthermore, RNA-seq analysis has revealed that organoids cultured using two distinct methods exhibit a heterogeneous cellular composition, comprising a total of 20 cell types (endothelial, immune cells ...). Our studies show that both methods successfully maintained the essential characteristics of GBM, encompassing its distinctive tissue structure and gene expression patterns. Each method exhibits its own attributes, contributing to the understanding of GBM organoids.

KEYWORDS

glioblastoma (GBM), organoids, patient-derived models, RNA sequencing, heterogeneity

Introduction

Glioblastoma (GBM) is the most common high-grade primary malignant brain tumor in adults. This tumor is characterized by its highly invasive nature, widespread heterogeneity, and has a poor prognosis, with a median survival period typically not exceeding two years^[1]. Despite recent progress in GBM research, there is still no curative treatment. Comprehensive therapeutic approaches such as surgical resection, radiotherapy, and chemotherapy can only marginally prolong patients' survival times^[2,3]. Therefore, GBM remains a significant challenge in the field of neuro-oncology.

Traditional two-dimensional (2D) cell lines hold substantial value for disease research^[4,5]. However, these models are

constrained by their inability to fully replicate the complexity and three-dimensional architecture of *in vivo* tissues. They may not accurately reflect the dynamic and spatially organized microenvironments found in real tissues, potentially leading to a reduced predictive accuracy of therapeutic responses. In recent years, organoid research has received widespread attention and development, and organoids have significant advantages over traditional 2D cell lines in retaining complexity and heterogeneity of the original tumor^[6-8]. Many studies have shown that organoid models exhibit sensitivities to targeted therapies or radiation that are similar to those of tumors in the body^[9,10], demonstrating significant potential in drug screening^[11,12]. For instance, the breast cancer organoids established by Norman Sachs and colleagues have successfully retained the histological and genetic

© The Author(s) 2024. Published by Tsinghua University Press. The articles published in this open access journal are distributed under the terms of the Creative Commons Attribution 4.0 International License (<http://creativecommons.org/licenses/by/4.0/>), which permits use, distribution and reproduction in any medium, provided the original work is properly cited.

*Address correspondence to Chunhui Cai, caichunhui@lishengbiotech.com; Xinxin Han, xxhan@sibs.ac.cn

Cite this article as Zhang, J., et al. *Cell Organoid*, 2024, 1: 9410004.

characteristics of the original tumors^[13]. The observation that the organoids' drug responses corresponded with the patients' responses underscores the potential of organoids as predictive *in vitro* models. Currently, an increasing number of organoid models are being developed to simulate various tumors, such as ovarian, pancreatic, and liver tumors^[14–16]. These organoid models provide more reliable experimental evidence for studying the occurrence, development, and treatment of tumor. With the continuous development and optimization of organoid technology, more breakthroughs in the field of biomedicine are expected in the future.

GBM exhibits extensive inter- and intratumor heterogeneity, which hinders in-depth investigations into the pathogenesis of GBM and impacts the development of effective treatment strategies^[17]. Existing models often struggle to capture the intricacies of GBM. Consequently, there is a pressing need for the development of more sophisticated models that can better reflect these complexities. GBM organoids can better simulate the heterogeneity and complexity of GBM^[18–21]. For example, Jeremy Rich derived organoids from patient GBM tissue and characterized the stem cell heterogeneity and hypoxia gradients^[18]; Fadi Jacob and colleagues have developed an innovative method to quickly establish GBM organoids from tumor tissue without dissociating the tumor tissue into single cells. The organoids derived from this method retain a significant degree of heterogeneity, gene expression profiles, and mutational characteristics of the original tumor cells^[19]. These organoids are expected to provide powerful tools for in-depth study of GBM pathogenesis, drug responses, and treatment strategies. Despite recent significant progress in the development of GBM organoid, there are still some limitations that need to be resolved. Such as immune response deficiencies and the absence of a vascular system, as well as debates regarding structural and genetic fidelity^[22,23]. Consequently, the development of novel GBM organoids is crucial for a deeper understanding of the biological characteristics of this disease.

In this study, we generated organoid using surgical samples from four patients with GBM. This method does not require the dissociation of tissue into single cells, nor the addition of matrix gel. To avoid necrosis in the core of the organoids, we adopted two methods to reduce the size of the organoids: One is to mechanically fragment the organoids, resulting in smaller pieces, and the other is enzymatic digestion of the organoids into single cells. To enhance our understanding of the characteristics of each method, we conducted photography, pathological staining, and RNA-seq analysis. Our results demonstrated that the organoids could preserve the key features of GBM and a portion of the tumor microenvironment. Furthermore, we observed heterogeneity among organoids derived from different patients. In summary, both methods provide insights for organoid research.

Results

Generation of GBM organoids without Matrigel and enzymes

With the full informed consent of the patients, we processed fresh surgically resected GBM tissue samples from four patients. In contrast to the conventional method of digesting tissue into single cells for organoid generation, we adopted a simplified method:

Initially, the GBM tissue was meticulously washed with a tissue irrigation buffer to eliminate contaminants, ensuring the sterility of subsequent experiments. Subsequently, the tissue was manually cut into small pieces approximately 1 mm³ in size using ophthalmic scissors. These pieces were directly mixed into organoid medium (without Matrigel) to facilitate *in vitro* growth. This simplified method is designed to promote organoid formation more efficiently. Typically, these small tissue pieces can generate organoids within approximately 2 weeks. To avoid necrosis in the core of the organoids, we adopted 2 methods to reduce the size of the organoids. As shown in Fig. 1a, we first treated the surgical tissue from four patients using the method and successfully generated GBM organoids. Subsequently, we subjected some of these organoids to RNA-seq analysis and divided the remaining organoids into 2 groups: one group underwent mechanical fragmentation into smaller pieces (Group 1), while the other was enzymatically digested to obtain a single-cell suspension (Group 2). Both groups were seeded into low attachment six-well plates (with three replicate wells each) and continued to be cultured. On the third post-inoculation (Day 2), we observed the formation of GBM organoids with a diameter of approximately 200 μm in Group 2, partial organoid samples from all groups were collected simultaneously for RNA-seq analysis. After 14 days, we collected all groups of organoids, with some used for pathological staining and others for RNA-seq.

The growth of GBM organoids

To monitor the development of the organoids, we performed serial photography. Organoids generated from tissue pieces demonstrated favorable growth characteristics. Initially, the edges of these small pieces were distinct. After 2 weeks in culture, the organoids' edges became smooth and even, with cells observed to proliferate outward (Fig. 1b). On the third day post-inoculation (Day 2), cells from Group 2 had formed numerous small organoids. Over time, these organoids increased in size and began to merge with adjacent organoids, resulting in larger, diversely shaped organoids (Figs. 2a and 2c). It is worth noting that the organoids within this group exhibited a small volume difference, with a relative increase in volume ranging from 2 to 5 times (Fig. 3a). However, Group 2-2, after forming organoids with a diameter of approximately 200 μm, did not exhibit significant growth changes during subsequent cultivation, and the specific reasons for this observation are yet to be elucidated. In contrast, the organoids from Group 1, which started with larger volumes, showed a relatively mild growth trend. These organoids gradually proliferate and grow, and have undergone fusion, resulting in the formation of organoids with diverse shapes. (Figs. 2a and 2b). It was encouraging to observe that some Group 1 organoids displayed clear vascular structures (Fig. 1c), although there was a significant variation in the volume of organoids within the group (Fig. 3a). To better summarize the growth characteristics of organoids, we conducted a detailed statistical analysis of the number of organoids (Fig. 3b), the maximum volume of organoids in each group (Fig. 3c), and the number of organoids exceeding a volume of 200,000 μm² (Fig. 3d). The results show that, during the early stages of organoid cultivation, there was a higher abundance of organoids with relatively smaller volumes. As the cultivation period progressed, the total number of organoids decreased, while the volume of organoids increased, and the count of larger organoids also rose.

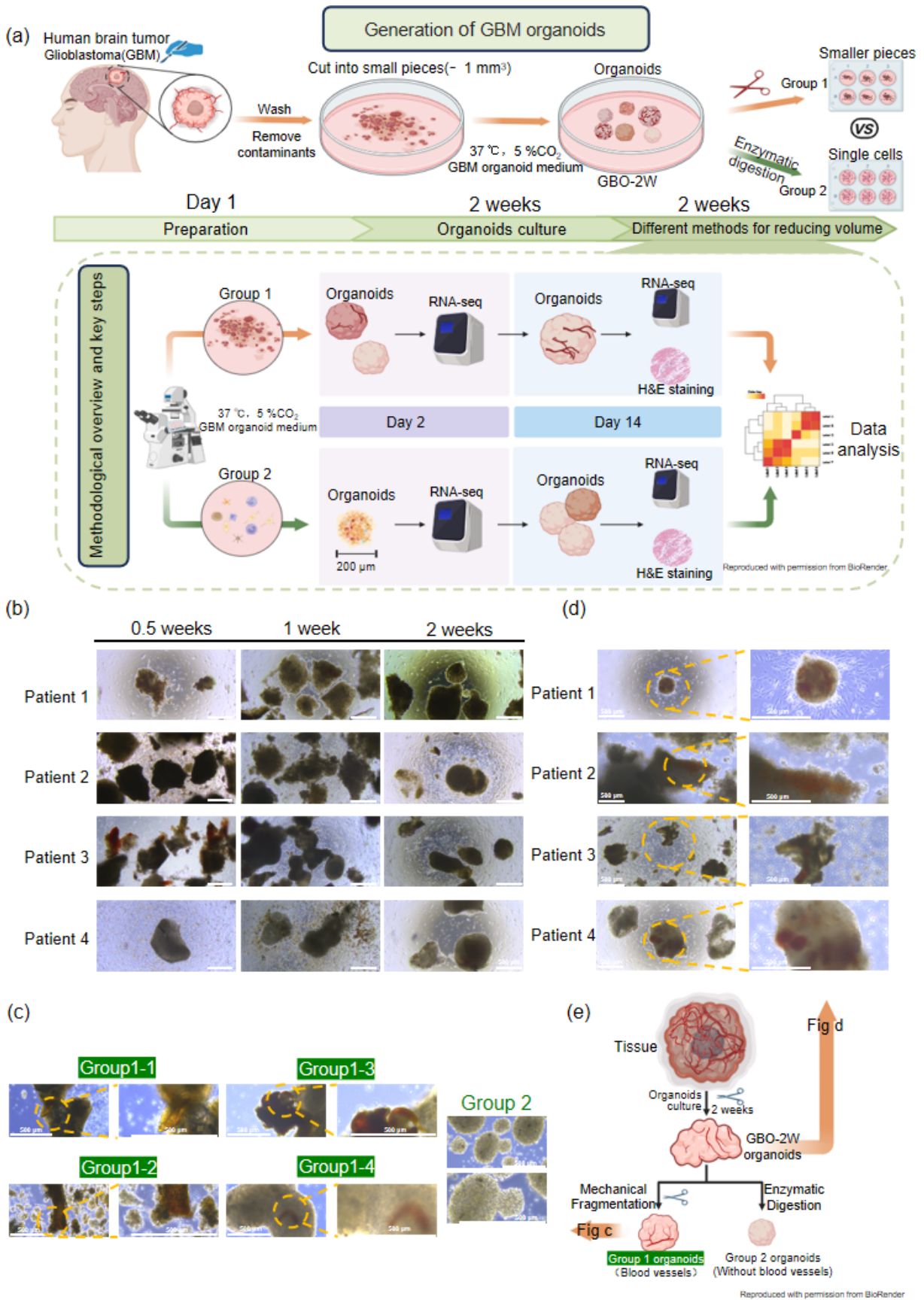


Figure 1. Generation of GBM organoids. (a) Methodological overview and key steps. (b) Brightfield microscopy images of organoid GBO-2W (organoids generated after 2 weeks of tissue culture) derived from tissue; scale bar = 500 μm. (c) Organoids with vascular structures (Group 1); Scale bar = 500 μm. (d) Organoids with vascular structures (GBO-2W); scale bar = 500 μm. (e) Schematic diagram of organoid characteristics across groups.

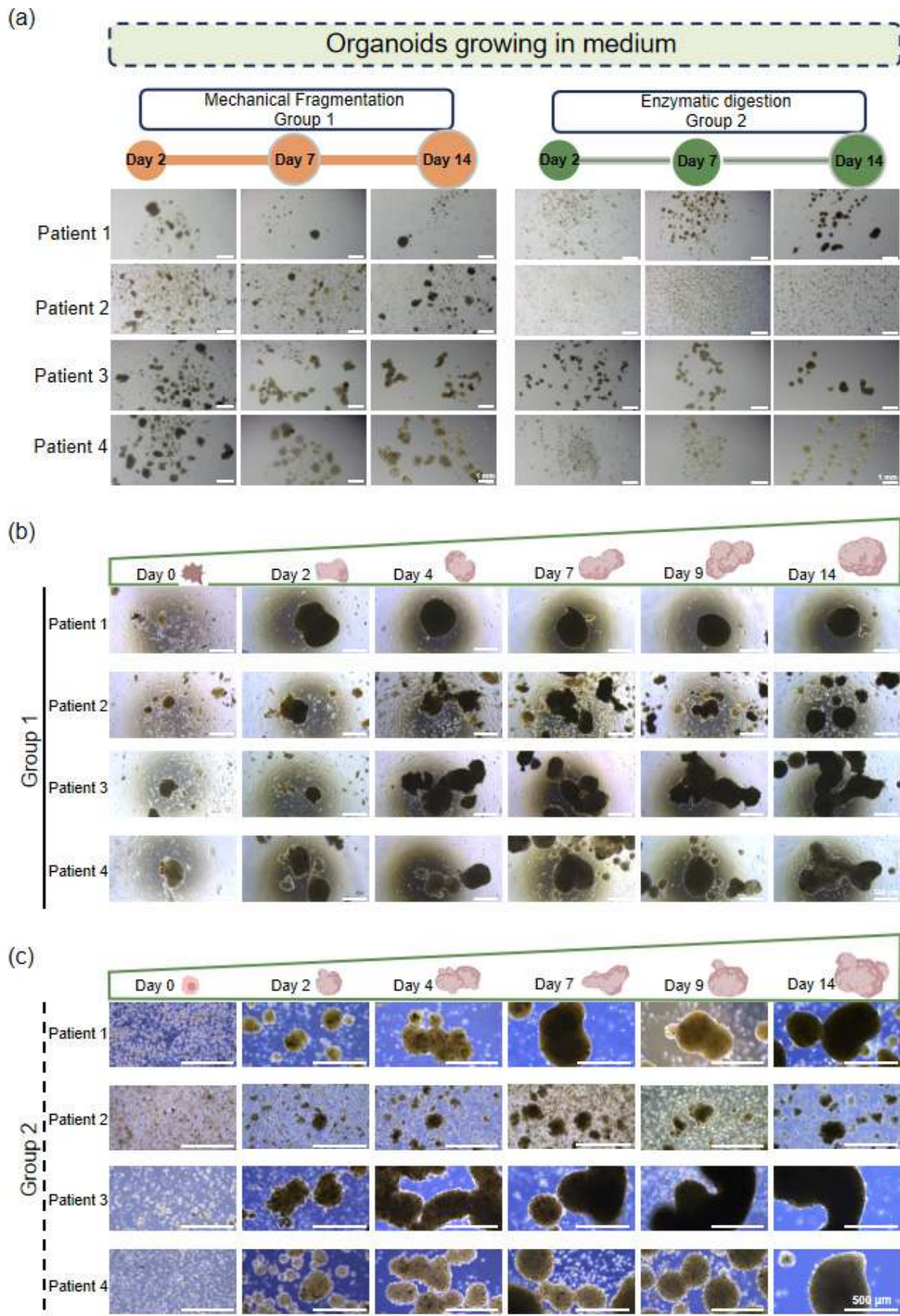
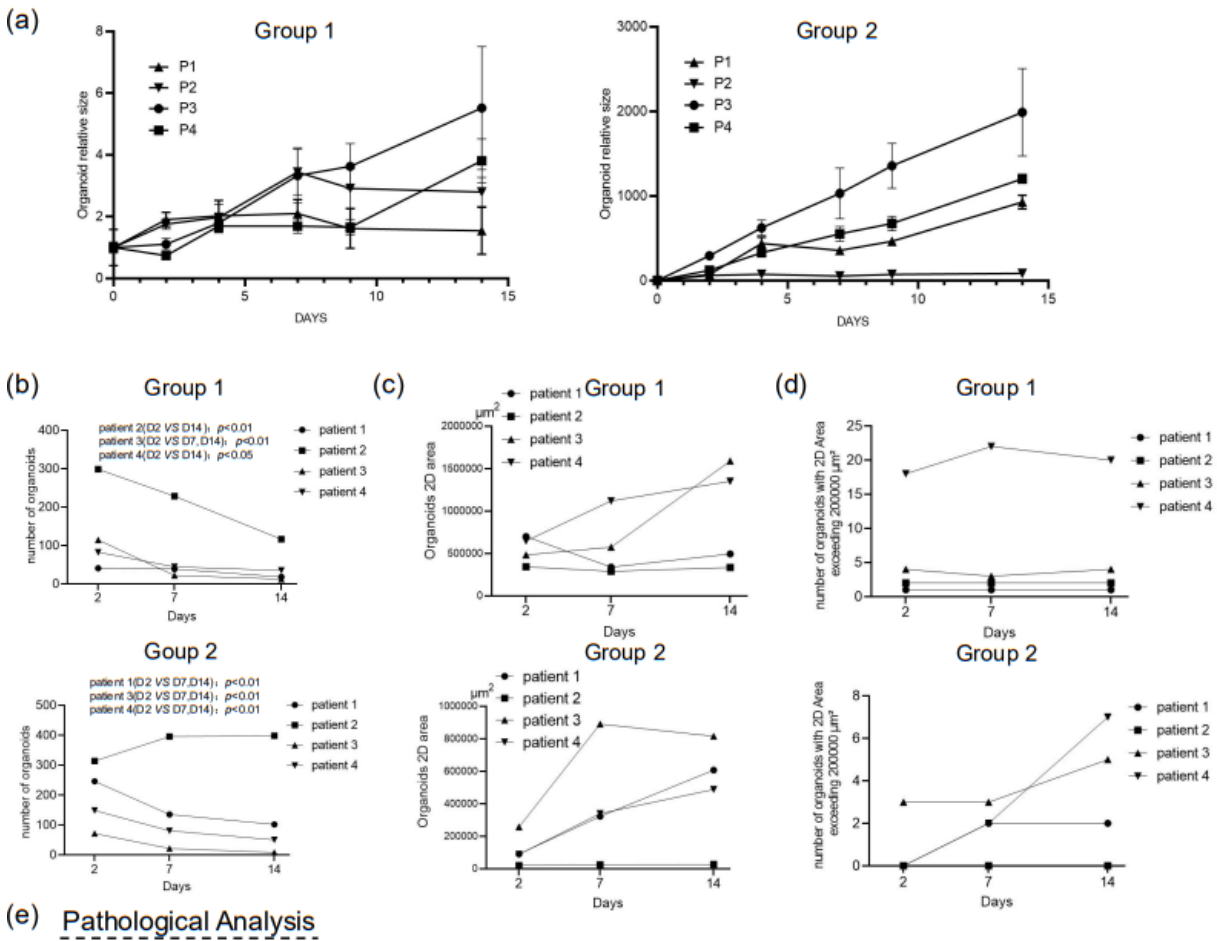


Figure 2. Growth record of organoids. (a) Organoid growth panorama; scale bar = 500 μm. (b) Brightfield microscopy images of Group 1; Scale bar = 500 μm. (c) Brightfield microscopy images of Group 2; scale bar = 500 μm.



(e) Pathological Analysis

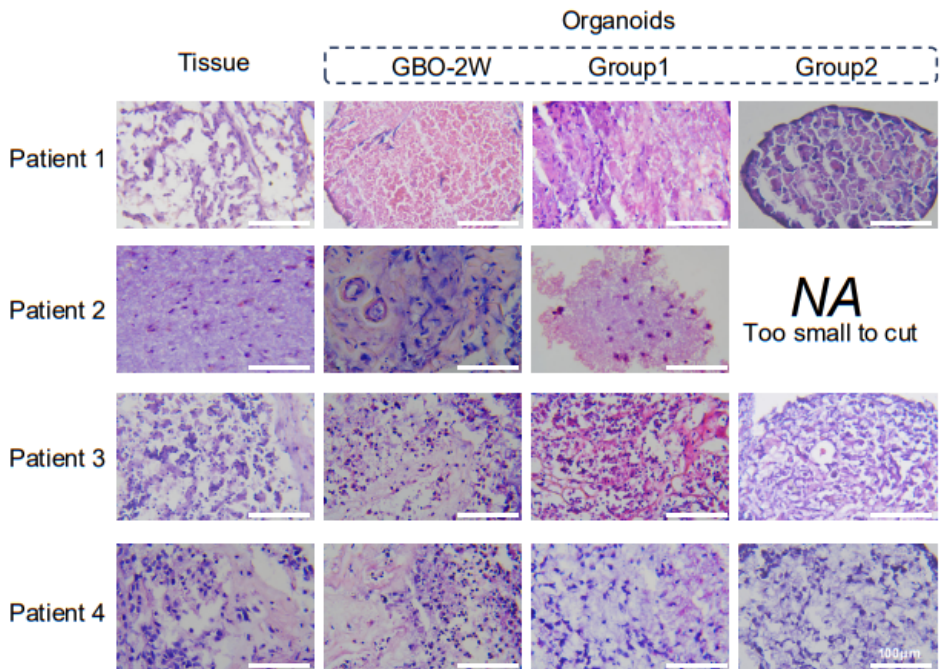


Figure 3. Growth record statistics chart and H&E staining results. (a) The statistics chart of organoid relative size. (b) The quantitative statistics chart of organoids. (c) The 2D area statistics chart of the largest organoids per group. (d) The statistical chart of the number of organoids with 2D area exceeding 200,000 μm². (e) Pathological analysis (H&E staining); Scale bar = 100 μm.

Histological characterization of GBM organoids

Hematoxylin and Eosin (H&E) staining is a commonly used

histological technique that clearly reveals the morphological structure of tissues and cells. Analysis of the organoids and their matched tissues after H&E staining revealed that our organoids

closely resembled their parental tumors in tissue morphology and exhibited typical features of GBM. In the organoid sections, dense clusters of tumor cells with irregular shapes and varying sizes were observed. The nuclei were enlarged, irregular in shape, and exhibited uneven chromatin distribution. Binucleation or multinucleation was also observed. Additionally, necrotic features characteristic of GBM, such as pseudopalisading, were observed in the organoids from patients 3 and 4, designated as GBO-2W (Fig. 3c).

Transcriptome Characterization of GBM Organoids

RNA sequencing (RNA-seq) technology was employed to elucidate the dynamics of gene expression during disease progression. To confirm whether organoids retained key characteristics of GBM, bulk RNA-seq analysis was conducted on organoids from Groups 1 and 2, encompassing two time points (Days 2 and 14), as well as organoids at the GBO-2W (Organoids generated after 2 weeks of tissue culture) stage (Fig. 4a). Utilizing a panel of cell markers to distinguish various cell populations within the neural tissue (Fig. 5a), our results showed that organoids derived from Patient 1 exhibited pronounced expression of genes related to the immune and vascular systems. In contrast, organoids from Patient 3 showed significant expression of genes associated with astrocytes and cell proliferation. Organoids from Patients 2 and 4 displayed elevated expression of genes related to astrocytes, immune cells, oligodendrocyte precursor cells, angiogenesis, and cell cycle regulation. The organoids from the four patients exhibited a rich diversity of cell types, including tumor cells, immune cells, and vascular-related cells (Fig. 4c). Moreover, the organoids from different patients exhibited significant transcriptional differences, which were further confirmed by principal component analysis (PCA) (Fig. 4d). Notably, organoids from the same patient source in Groups 1 and 2 at the two time points (Days 2 and 14) demonstrated a high degree of similarity in cell composition to the GBO-2W organoids, with the proportion of various cell types remaining relatively stable over time (Fig. 5b). Correlation analysis further indicated a high level of transcriptional consistency among organoids from different groups of the same patient source (Fig. 4b).

The tumor immune microenvironment plays a crucial role in tumor growth and progression. To investigate the dynamic changes in the immune microenvironment within organoids, we analyzed the RNA-seq data. The results showed that the proportions of various immune cells in Groups 1 and 2 remained strikingly similar across different time points (Fig. 5b), with monocytes consistently maintaining a high proportion. Further analysis of the proportion of each immune cell type revealed that the immune cell composition in Groups 1 and 2 did not undergo significant changes over time (Fig. 5d). Additionally, it was observed that the endothelial cell population in both Groups 1 and 2 did not exhibit significant changes over time (Fig. 5c).

Discussion

Traditional GBM cell lines, including U87, U251, and GL261, have played a pivotal role in medical research, providing a foundational experimental platform for elucidating disease mechanisms, and conducting drug screening^[24,25]. However, these cell lines are limited by their inability to accurately replicate the three-dimensional architecture and heterogeneity of tumors^[26,27]. In

contrast, GBM organoid models offer a more authentic representation of tumors, providing a more precise experimental platform for studying cellular interactions, immune cell dynamics, and drug responses^[18,19,28].

In this study, we successfully generated organoids from GBM tissue resected from patients. HE staining showed that these organoids retained the typical histological features of GBM. RNA-seq confirmed that the organoids maintained GBM-specific gene expression profiles. Cell type analysis demonstrated the diversity of cells within the organoids. Previous studies have shown significant heterogeneity among GBM patients^[29], a characteristic that was reflected in our organoids. The organoids derived from tumor tissues of various patients demonstrated a notable diversity in their transcriptional profiles. Unlike other methods for generating organoids from patient-derived tissues, our methods circumvent the need for dissociating tumor tissue into single cells and does not employ the use of Matrigel.

The generation of organoids from tissue pieces typically takes about two weeks. As organoids increase in size, larger ones may experience hypoxia and nutrient deprivation in their central regions, leading to cell apoptosis and necrosis. To overcome this limitation, we adopted two methods—enzymatic digestion and mechanical fragmentation—to reduce the organoids' size. Encouragingly, after enzymatic digestion, the dissociated single cells exhibited the capacity to self-assemble into new organoids without the supplementation of any extracellular matrigel. Both H&E staining and RNA sequencing analysis showed that organoids treated with enzymatic digestion (Group 1) and mechanical fragmentation (Group 2) successfully retained the typical histological features and gene expression profiles of GBM. Additionally, organoids from both treatment methods showed a significant similarity in transcriptome and cell diversity to the GBO-2W organoids. Photography records indicated that the mechanical fragmentation tended to preserve some of the original tissue's architecture, while the enzymatic digestion required cells to re-establish interactions during the cultivation process, which might have resulted in the loss of the original tissue structure. However, enzymatic digestion leads to the formation of uniformly sized organoids. Both methods have their advantages in the cultivation of patient-derived organoids. Mechanical fragmentation may be suitable for experiments requiring the preservation of the original tissue structure, while enzymatic digestion may be more appropriate for studying the process of cellular tissue remodeling.

Tumors are complex ecosystems composed of various cell types, not just tumor cells, but also including multiple non-tumor cell types^[30]. Our organoids also contained other non-tumor cell types, such as endothelial cells, mural cell and immune cells. Significantly, the relative proportions of these cell types remained stable throughout the cultivation process. The tumor immune microenvironment plays a pivotal role in tumor development, and researchers are continuously optimizing organoid culture techniques to mimic the immune response more accurately within tumors^[31–33]. Currently, two main strategies are employed: one involves retaining and expanding the original immune cells within the organoids, and the other involves introducing new immune cells into the organoid culture system^[34]. We have paid particular attention to the retention of immune cells during the organoid culture process and found that our culture system effectively maintained the immune microenvironment in both Groups 1 and 2.

Although we successfully generated organoids that reflect

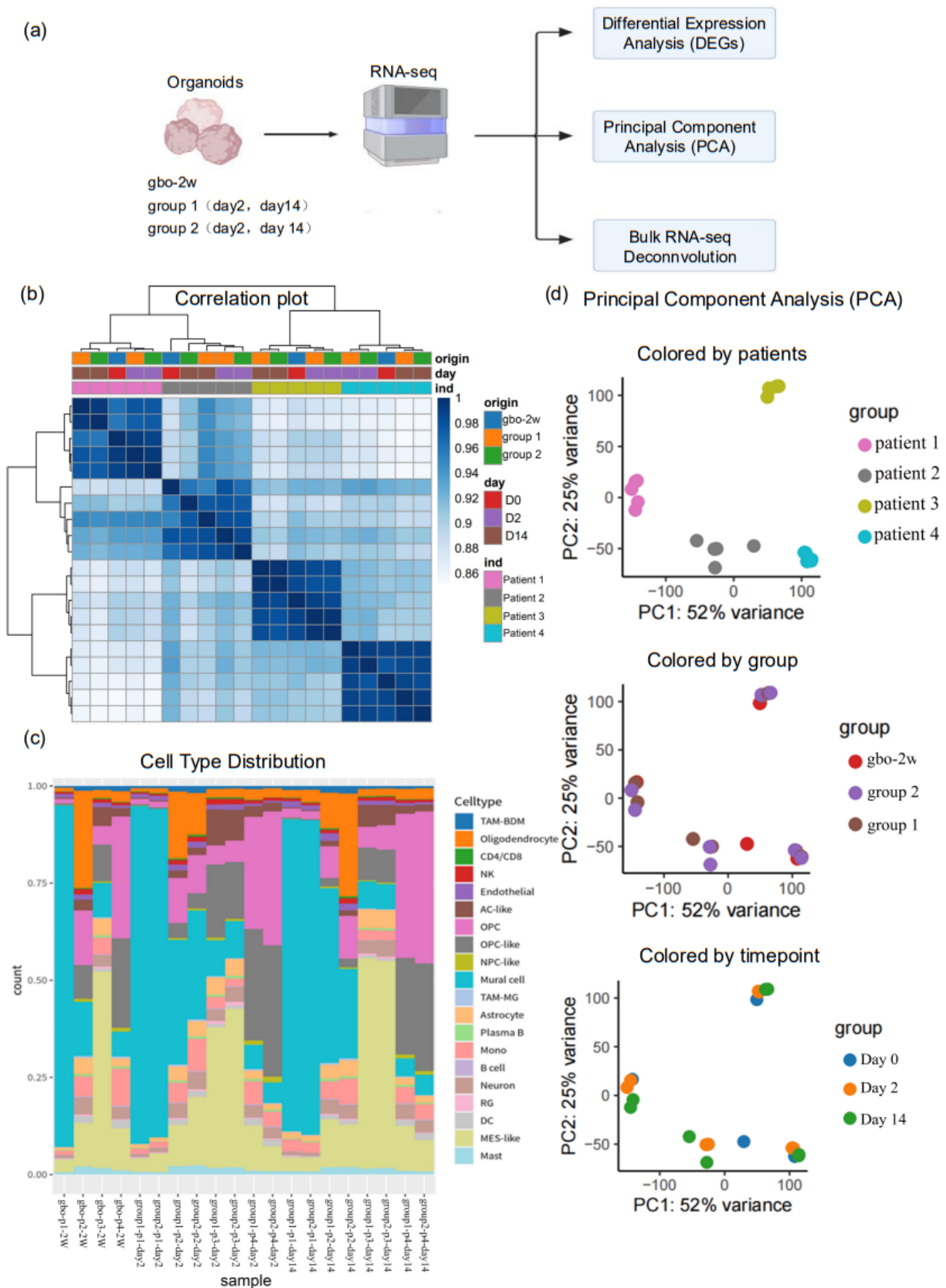


Figure 4. Bulk RNA-Seq analysis of organoids. (a) The workflow for Bulk RNA-Seq analysis. (b) Correlation analysis. (c) Cell type distribution. (d) Principal component analysis.

typical GBM features and partially retain the immune microenvironment, our study still faces some limitations. The

scarcity of GBM patient tissue, coupled with their small volume, limits the number of organoids we can generate. In this

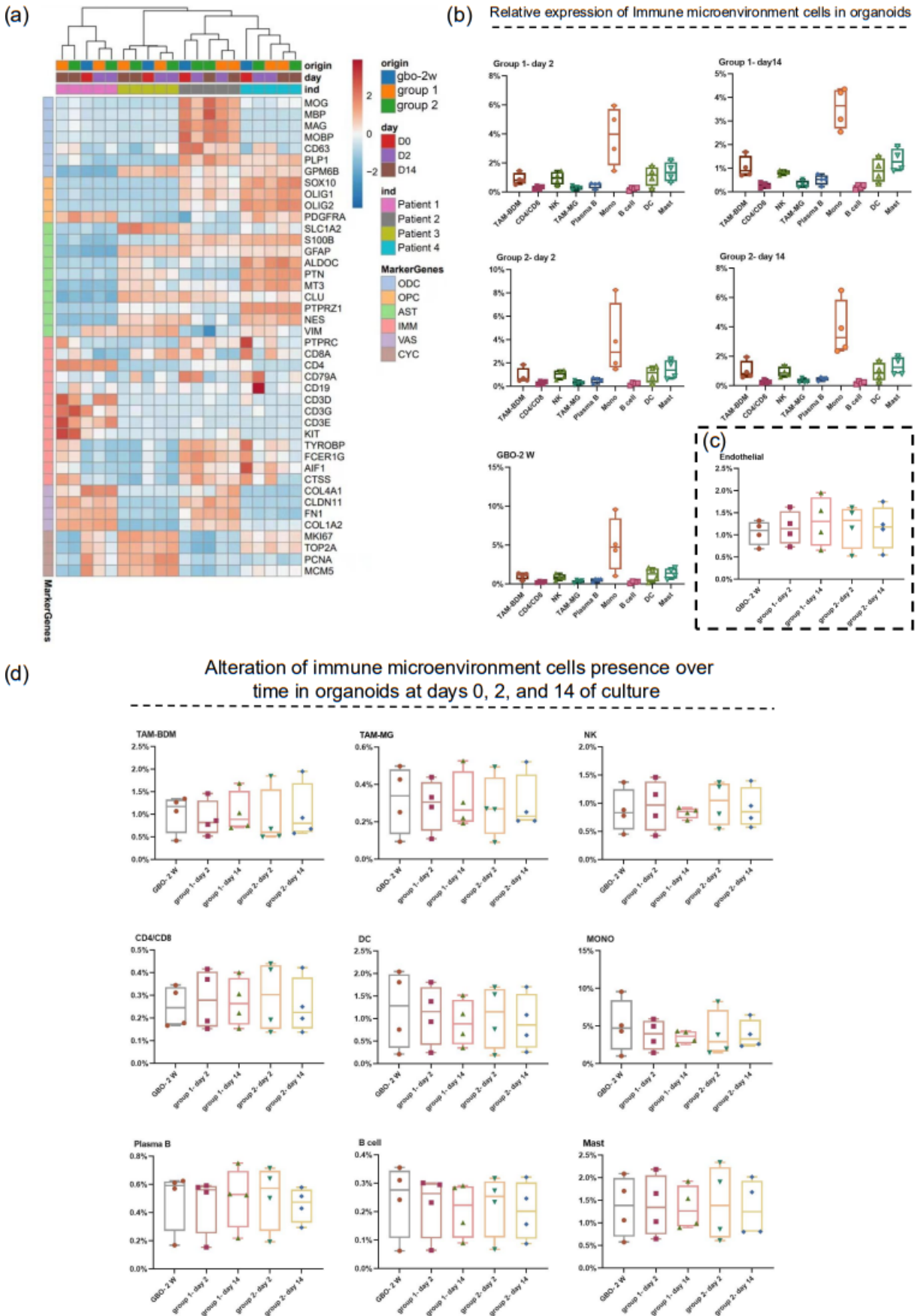


Figure 5. Cell type-specific molecular markers in organoids and RNA-Seq analysis of the immune microenvironment. (a) Cell type-specific molecular marker expression analysis. (b) Relative expression of immune microenvironment cells in organoids. (c) Alteration of immune microenvironment cells presence over time in organoids at Days 0, 2, and 14 of culture.

experiment, we generated organoids from GBM tissue of only four patients. Moreover, despite adopting some histological staining and RNA-seq analysis, the limited number of organoid samples may not fully reveal the characteristics of our GBM organoids. Therefore, enhancing the efficiency of organoid generation and delving into a more comprehensive analysis of their characteristics will be central to our upcoming research endeavors.

In summary, our study shows the characteristics of mechanical fragmentation and enzymatic digestion within the organoid cultivation process, which may offer a preliminary reference for future research in this area. Furthermore, it is advisable for researchers to take into account their research objectives and specific needs when choosing a suitable cultivation method.

Methods and materials

Tissue collection

We strictly adhere to ethical norms and standard operating procedures in the collection of clinical tissue samples, ensuring the integrity and quality of the samples. The main steps include: identifying patients, obtaining informed consent, collecting samples, processing samples, storage, and documentation. All sample collection work is carried out by professionally trained medical personnel following prescribed procedures to reduce the risk of sample contamination, ensure the viability of the samples, and facilitate subsequent analysis. At the same time, we also implement strict record-keeping and label management systems to ensure the traceability of samples and facilitate accurate data management. In the collection of all clinical samples, we strictly adhered to the ethical guidelines of the Xinhua Hospital Affiliated to Shanghai Jiao Tong University School of Medicine and the ethical code XHEC-D-2024-019.

Organoid culture

In this study, we employed a standardized protocol for processing fresh GBM tissue samples to generate organoids. First, freshly obtained GBM tissue samples were immersed in a tissue irrigation buffer (LSNO00100201; Shanghai Lisheng Biotech, China) for 3 min to eliminate potential contaminants and non-cellular debris. The tissue samples were then transferred to a 50 mL centrifuge tube and washed 3–5 times with fresh tissue irrigation buffer, each time adding 5–10 mL and gently agitating to ensure thorough cleansing. Following the washing steps, the tissue samples were placed into a 10 cm dish and infused with 100 μ L of medium (LSTO015004; Shanghai Lisheng Biotech, China). Utilizing ophthalmic scissors, the tissue samples were cut into micro-tissue pieces approximately 1 mm³ in size. After resuspending the micro-tissue pieces in 1 mL of medium, they were transferred to a new 10 cm dish for observation and further cultivation. Finally, 15 mL of medium was added, and the dish was incubated in an incubator at 37 °C with 5% CO₂ to facilitate growth.

During the organoid cultivation process, we replaced part of the medium every 5–7 days, or adjusted it in time according to the color and turbidity of the medium to ensure sufficient nutrition for the growth of organoids. We meticulously monitored and regulated the cultivation conditions throughout the process to guarantee the precision and reliability of our experimental outcomes.

Group 1: A portion of the GBO-2W organoids were aspirated

and transferred to a new 10 cm dish, with a minimal volume of liquid retained to preserve organoid hydration while excess medium was removed. The organoids were cut into smaller pieces using ophthalmic scissors. Subsequently, 6 mL of medium was added, and the organoid-laden medium was evenly distributed into low-adhesion 6-well plates. Throughout the cultivation process, the medium was consistently replenished every 5–7 days, and its composition was promptly adjusted based on its color and turbidity to ensure an optimal environment for organoid growth.

Enzymatic digestion

Group 2: An appropriate number of organoids was carefully taken, transferred to a 6-well plate, and allowed to settle at the bottom, with any excess supernatant being removed. Subsequently, 200 μ L of organoid dissociation reagent (LSNO00100501; Shanghai Lisheng Biotech, China) was added, and the organoids were cut into small pieces with ophthalmic scissors to facilitate enzymatic digestion. After adding 1 mL of organoid dissociation reagent and thoroughly mixing, the mixture was placed in an incubator and shaken for 20 min to complete the digestion process. The mixture was repeatedly aspirated with a 1 mL pipette to break up any visible clumps. If a noticeable resistance due to clogged particles was felt, the digestion was continued for an additional 10 min. The mixture was filtered through a 70 μ m cell strainer, and the strainer was rinsed with 2 mL of medium to collect a single-cell suspension. This suspension was then centrifuged (600 r/min, 10 min). After centrifugation, the supernatant was carefully removed, and the cells were resuspended in 2 mL of medium. This suspension underwent a second centrifugation at 600 r/min for 10 min. Following the second spin, the supernatant was again removed, and the cells were resuspended in 6 mL of fresh medium. This cell suspension was then evenly distributed into three replicate wells in a 6-well plate. The medium was routinely replenished every 5–7 days, with adjustments made as necessary based on the medium's color and turbidity to ensure a conducive culture environment.

Organoids growth analysis

In this study, we used ImageJ software to quantitatively analyze the size of the organoids, measuring the changes in size at different time points and continuously monitoring the growth and morphological changes of the organoids. These data provided important information for assessing the impact of experimental methods on organoid growth.

H&E staining

Tissue and organoids were fixed in 4% paraformaldehyde (PFA, BL539A, Biosharp) for 48 h, followed by gradient dehydration (1 h in 10%, 2 h in 20%, and overnight in 30% sucrose), then embedded in tissue-freezing medium (OCT) and rapidly frozen with liquid nitrogen. Section 10 micrometers thick were prepared using a microtome. Subsequently, H&E staining was performed according to the instructions provided with the H&E staining kit (G1120) from Solarbio (China).

RNA sequencing

After the collection of organoids, the samples were immediately placed on ice and treated with an adequate amount of TRIzol reagent for tissue lysis. The samples were then thoroughly homogenized using a disposable pestle to ensure complete

disruption of the tissue cells. The homogenate was carefully stored at -80°C in a low-temperature freezer to maintain sample integrity. Subsequently, the samples were sent to Shanghai HonSun Biological Technology Co., Ltd. for professional sequencing services to ensure the accuracy and quality of the analysis. The bulk RNA-seq data were processed using the kb Python package, a wrapper around kallisto and bustools. The reference genome and gene annotation files were sourced from 10x Genomics. A kallisto index was created for efficient transcript-to-gene mapping. The resulting count matrices were imported into R for normalization and differential gene expression analysis using the DESeq2 R package. PCA was performed on the variable gene matrix, selecting the top 50 components for further analysis. To correct for batch effects from different organoids, the harmony algorithm was employed. Cell clusters were defined using the Leiden algorithm on nearest neighbor graphs based on harmonized embedding. UMAP was used for visualization. Marker genes were identified using Scanpy's `rank_genes_groups` function with logistic regression (method='logreg') for up to 200 genes. Cluster markers were interpreted, and cluster identities were assigned based on known cell type annotations from literature, such as Astrocyte (SLC1A2, S100B, GFAP, ALDOC, PTN...), Cell Cycle (MKI67, TPO2A, PCNA, MCM5), Immune cell (PTPRC, CD8A, CD4, CD79A, CD19...), Oligodendrocyte/OPC (MOG, MBP, MAG, MOBP, SOX10, OLIG1, OLIG2, PDGFRA...), Vasculature (COL4A1, CLDN11, FN1, COL1A2).

Statistical analysis

Data were gathered from a minimum of three replicates, with the quantitative outcomes presented as the mean value accompanied by the standard deviation. The statistical analysis was executed utilizing GraphPad Prism 8.0.

Research ethics and patient consent

Clinical samples were collected in accordance with the ethical guidelines set forth by the Ethics Committee of Xinhua Hospital Affiliated with Shanghai Jiao Tong University School of Medicine. The study was granted ethical Approval No. XHEC-D-2024-019. Before donating samples, all participants provided informed consent, explicitly stating the intended use of their samples for future research. The voluntary participation and understanding of the study's objectives by the participants played a vital role in upholding ethical standards throughout the course of this research.

Availability of data and material

The data and materials that support the findings of this study are available from the corresponding author upon reasonable request.

Declaration of conflicting interests

This work was sponsored by Shanghai Lisheng Biotech Ltd (Lisheng). The manuscript was written in a responsible and ethical manner. X.X.H. is a shareholder of Lisheng, as a founder. Y.H.S., L.Y.L., C.W., J.Z., M.J.R., J.P.L. and C.H.C. are senior scientists of Lisheng.

X.X.H. and C.H.C. are members of the Editorial Board for Cell Organoid. They were not involved in the journal's review of, or decisions related to, this manuscript.

Author contributions

X.X.H., C.H.C. and J.Z. conceived and designed the study. Y.H.S., L.Y.L., C.W., M.J.R., B.B.T., H.T. and J. Z. collected the samples, and performed the experiments. J.P.L., C.H.C., X.X.H. and J.Z. analyzed the data. C.H.C., X.X.H., W.D. and J.Z. wrote the manuscript. All the authors read and approved the final version of the manuscript.

References

- [1] Schaff, L. R., Mellinghoff, I. K. Glioblastoma and other primary brain malignancies in adults: a review. *JAMA*, **2023**, 329(7): 574–587. <https://doi.org/10.1001/jama.2023.0023>
- [2] Ahluwalia, M. S., Reardon, D. A., Abad, A. P., Curry, W. T., Wong, E. T., Figel, S. A., Mechtler, L. L., Peereboom, D. M., Hutson, A. D., Withers, H. G. et al. Phase IIa study of SurVaxM plus adjuvant temozolomide for newly diagnosed glioblastoma. *Journal of Clinical Oncology*, **2023**, 41(7): 1453–1465. <https://doi.org/10.1200/jco.22.00996>
- [3] Tsien, C. I., Pugh, S. L., Dicker, A. P., Raizer, J. J., Matuszak, M. M., Lallana, E. C., Huang, J. Y., Algan, O., Deb, N., Portelance, L. et al. NRG oncology/RTOG1205: A randomized phase II trial of concurrent bevacizumab and reirradiation versus bevacizumab alone as treatment for recurrent glioblastoma. *Journal of Clinical Oncology*, **2023**, 41(6): 1285–1295. <https://doi.org/10.1200/jco.22.00164>
- [4] Gonçalves, E., Poulos, R. C., Cai, Z., Barthorpe, S., Manda, S. S., Lucas, N., Beck, A., Bucio-Noble, D., Dausmann, M., Hall, C., et al. Pan-cancer proteomic map of 949 human cell lines. *Cancer Cell*, **2022**, 40(8): 835–849. <https://doi.org/10.1016/j.ccell.2022.06.010>
- [5] Barretina, J., Caponigro, G., Stransky, N., Venkatesan, K., Margolin, A. A., Kim, S., J Wilson, C., Lehár, J., Kryukov, G. V., Sonkin, D. et al. Addendum: The Cancer Cell Line Encyclopedia enables predictive modelling of anticancer drug sensitivity. *Nature*, **2012**, 492(7428): 290. <https://doi.org/10.1038/nature11735>
- [6] Cowan, C. S., Renner, M., De Gennaro, M., Gross-Scherf, B., Goldblum, D., Hou, Y. Y., Munz, M., Rodrigues, T. M., Krol, J., Szikra, T., et al. Cell types of the human retina and its organoids at single-cell resolution. *Cell*, **2020**, 182(6): 1623–1640. <https://doi.org/10.1016/j.cell.2020.08.013>
- [7] Mo, S. B., Tang, P. Y., Luo, W. Q., Zhang, L., Li, Y. Q., Hu, X., Ma, X. J., Chen, Y. K., Bao, Y. C., He, X. F. et al. Patient-derived organoids from colorectal cancer with paired liver metastasis reveal tumor heterogeneity and predict response to chemotherapy. *Advanced Science*, **2022**, 9(31): e2204097. <https://doi.org/10.1002/adv.202204097>
- [8] Han, X. X., Cai, C. H., Deng, W., Shi, Y. H., Li, L. Y., Wang, C., Zhang, J., Rong, M. J., Liu, J. P., Fang, B. J. et al. Landscape of human organoids: Ideal model in clinics and research. *The Innovation*, **2024**, 5(3): 100620. <https://doi.org/10.1016/j.xinn.2024.100620>
- [9] Bian, S., Repic, M., Guo, Z. M., Kavirayani, A., Burkard, T., Bagley, J. A., Krauditsch, C., Knoblich, J. A. Genetically engineered cerebral organoids model brain tumor formation. *Nature Methods*, **2018**, 15(8): 631–639. <https://doi.org/10.1038/s41592-018-0070-7>
- [10] Gao, D., Vela, I., Sboner, A., Iaquinta, P. J., Karthaus, W. R., Gopalan, A., Dowling, C., Wanjala, J. N., Undvall, E. A., Arora, V. K. et al. Organoid cultures derived from patients with advanced prostate cancer. *Cell*, **2014**, 159(1): 176–187. <https://doi.org/10.1016/j.cell.2014.08.016>
- [11] Drost, J., van Jaarsveld, R. H., Ponsioen, B., Zimmerlin, C., van Boxtel, R., Buijs, A., Sachs, N., Overmeer, R. M., Offerhaus, G. J., Begthel, H. et al. Sequential cancer mutations in cultured human intestinal stem cells. *Nature*, **2015**, 521(7550): 43–47. <https://doi.org/10.1038/nature14415>

- [12] Broutier, L., Mastrogianni, G., Versteegen, M. M., Francies, H. E., Gavarró, L. M., Bradshaw, C. R., Allen, G. E., Arnes-Benito, R., Sidorova, O., Gaspersz, M. P. et al. Human primary liver cancer-derived organoid cultures for disease modeling and drug screening. *Nature Medicine*, **2017**, 23(12): 1424–1435. <https://doi.org/10.1038/nm.4438>
- [13] Sachs, N., de Ligt, J., Kopper, O., Gogola, E., Bounova, G., Weeber, F., Balgobind, A. V., Wind, K., Gracanin, A., Begthel, H. et al. A living biobank of breast cancer organoids captures disease heterogeneity. *Cell*, **2018**, 172(1–2): 373–386.e10. <https://doi.org/10.1016/j.cell.2017.11.010>
- [14] Kopper, O., de Witte, C. J., Löhmußaar, K., Valle-Inclan, J. E., Hami, N., Kester, L., Balgobind, A. V., Korving, J., Proost, N., Begthel, H. et al. An organoid platform for ovarian cancer captures intra- and interpatient heterogeneity. *Nature Medicine*, **2019**, 25(5): 838–849. <https://doi.org/10.1038/s41591-019-0422-6>
- [15] Boj, S. F., Hwang, C. I., Baker, L. A., Chio, I. I., Engle, D. D., Corbo, V., Jager, M., Ponz-Sarvisé, M., Tiriác, H., Spector, M. S. et al. Organoid models of human and mouse ductal pancreatic cancer. *Cell*, **2015**, 160(1–2): 324–338. <https://doi.org/10.1016/j.cell.2014.12.021>
- [16] Mun, S. J., Ryu, J. S., Lee, M. O., Son, Y. S., Oh, S. J., Cho, H. S., Son, M. Y., Kim, D. S., Kim, S. J., Yoo, H. J. et al. Generation of expandable human pluripotent stem cell-derived hepatocyte-like liver organoids. *Journal of Hepatology*, **2019**, 71(5): 970–985. <https://doi.org/10.1016/j.jhep.2019.06.030>
- [17] Andersen, B. M., Faust, A. C., Wheeler, M. A., Chiocca, E. A., Reardon D. A., Quintana, F. J. Glial and myeloid heterogeneity in the brain tumour microenvironment. *Nature Review Cancer*, **2021**, 21(12): 786–802. <https://doi.org/10.1038/s41568-021-00397-3>
- [18] Hubert, C. G., Rivera, M., Spangler, L. C., Wu, Q. L., Mack, S. C., Prager, B. C., Couce, M., McLendon, R. E., Sloan, A. E., Rich, J. N. A three-dimensional organoid culture system derived from human glioblastomas recapitulates the hypoxic gradients and cancer stem cell heterogeneity of tumors found *in vivo*. *Cancer Research*, **2016**, 76(8): 2465–2477. <https://doi.org/10.1158/0008-5472.can-15-2402>
- [19] Jacob, F., Salinas, R. D., Zhang, D. Y., Nguyen, P. T. T., Schnoll, J. G., Wong, S. Z. H., Thokala, R., Sheikh, S., Saxena, D., Prokop, S. et al. A patient-derived glioblastoma organoid model and biobank recapitulates inter- and intra-tumoral heterogeneity. *Cell*, **2020**, 180(1): 188–204.e22. <https://doi.org/10.1016/j.cell.2019.11.036>
- [20] Ogawa, J., Pao, G., Shokhirev, M., Verma, I. Glioblastoma model using human cerebral organoids. *Cell Reports*, **2018**, 23(4): 1220–1229. <https://doi.org/10.1016/j.celrep.2018.03.105>
- [21] Ratliff, M., Kim, H., Qi, H., Kim, M., Ku, B., Azorin, D. D., Hausmann, D., Khajuria, R. K., Patel, A., Maier, E., et al. Patient-derived tumor organoids for guidance of personalized drug therapies in recurrent glioblastoma. *International Journal of Molecular Sciences*, **2022**, 23(12): 6572. <https://doi.org/10.3390/ijms23126572>
- [22] Silvia, V., Kedaigle Amanda, J., Simmons Sean, K., Allison, N., Marina, R., Giorgia, Q., Bruna, P., Lan, N., Xian, A., Aviv, R. et al. Individual brain organoids reproducibly form cell diversity of the human cerebral cortex. *Nature*, **2019**, 570(7762): 523–527. <https://doi.org/10.1038/s41586-019-1289-x>
- [23] Zhang, C. C., Jin, M. Z., Zhao, J. N., Chen, J. X., Jin, W. L. Organoid models of glioblastoma: Advances, applications and challenges. *American Journal of Cancer Research*, **2020**, 10(8): 2242–2257.
- [24] Qiu, G.-Z., Mao, X.-Y., Ma, Y., Gao, X.-C., Wang, Z., Jin, M.-Z., Sun, W., Zou, Y.-X., Lin, J., Fu, H.-L., et al. Ubiquitin-specific protease 22 acts as an oncoprotein to maintain glioma malignancy through deubiquitinating b cell-specific moloney murine leukemia virus integration site 1 for stabilization. *Cancer Science*, **2018**, 109(7): 2199–2210. <https://doi.org/10.1111/cas.13646>
- [25] Li, H., Chen, L., Li, J. J., Zhou, Q., Huang, A. N., Liu, W. W., Wang, K., Gao, L., Qi, S. T., Lu, Y. T. MiR-519a enhances chemosensitivity and promotes autophagy in glioblastoma by targeting STAT3/Bcl2 signaling pathway. *Journal of Hematology & Oncology*, **2018**, 11(1): 70. <https://doi.org/10.1186/s13045-018-0618-0>
- [26] Allen, M., Bjerke, M., Edlund, H., Nelander, S., Westermark, B. Origin of the u87mg glioma cell line: good news and bad news. *Science Translation Medicine*, **2016**, 8(354): 354re3. <https://doi.org/10.1126/scitranslmed.aaf685>
- [27] Da Hora, C. C., Schweiger, M. W., Wurdinger, T., Tannous, B. A. Patient-derived glioma models: from patients to dish to animals. *Cells*, **2019**, 8(10): 1177. <https://doi.org/10.3390/cells8101177>
- [28] Krieger, T., Tirier, S., Park, J., Eisemann, T., Peterziel, H., Angel, P., Eils, R., Conrad, C. Modeling glioblastoma invasion using human brain organoids and single-cell transcriptomics. *Neuro-Oncology*, **2020**, 22(8): 1138–1149. <https://doi.org/10.1093/neuonc/noaa091>
- [29] Nefel, C., Laffy, J., Filbin, M. G., Hara, T., Shore, M., Shore, M., Rahme, G., Rahme, G., Richman, A. R., Richman, A. R. et al. An integrative model of cellular states, plasticity, and genetics for glioblastoma. *Cell*, **2019**, 178(4): 835–849. <https://doi.org/10.1016/j.cell.2019.06.024>
- [30] Pitt, J. M., Marabelle, A., Eggermont, A., Soria, J. C., Kroemer, G., Zitvogel, L. Targeting the tumor microenvironment: Removing obstruction to anticancer immune responses and immunotherapy. *Annals of Oncology*, **2016**, 27(8): 1482–1492. <https://doi.org/10.1093/annonc/mdw168>
- [31] Jin, M. Z., Jin, W. L. The updated landscape of tumor microenvironment and drug repurposing. *Signal Transduction and Targeted Therapy*, **2020**, 5: 166. <https://doi.org/10.1038/s41392-020-00280-x>
- [32] Tang, H. D., Qiao, J., Fu, Y.-X. Immunotherapy and tumor microenvironment. *Cancer Letters*, **2016**, 370(1): 85–90. <https://doi.org/10.1016/j.canlet.2015.10.009>
- [33] Fu, T., Dai, L. J., Wu, S. Y., Xiao, Y., Ma, D., Jiang, Y. Z., Shao, Z. M. Spatial architecture of the immune microenvironment orchestrates tumor immunity and therapeutic response. *Journal of Hematology & Oncology*, **2021**, 14(1): 98. <https://doi.org/10.1186/s13045-021-01103-4>
- [34] Grönholm, M., Feodoroff, M., Antignani, G., Martins, B., Hamdan, F., Cerullo, V. Patient-derived organoids for precision cancer immunotherapy. *Cancer Research*, **2021**, 81(12): 3149–3155. <https://doi.org/10.1158/0008-5472.CAN-20-4026>